Structure–Function Analysis of the TssL Cytoplasmic Domain Reveals a New Interaction between the Type VI Secretion Baseplate and Membrane Complexes

Abdelrahim Zoued[1], Chloé J. Cassaro[1], Eric Durand[1], Badreddine Douzi[2,3], Alexandre P. España[1], Christian Cambillau[2,3], Laure Journet[1] and Eric Cascales[1]

*1 - **Laboratoire d'Ingénierie des Systèmes Macromoléculaires (LISM,** UMR 7255), Institut de Microbiologie de la Méditerranée (IMM), Aix-Marseille Univ. - Centre National de la Recherche Scientifique (CNRS), 31 Chemin Joseph Aiguier, 13402 Marseille Cedex 20, France*

*2 - **Architecture et Fonction des Macromolécules Biologiques (AFMB,** UMR 6098), Centre National de la Recherche Scientifique (CNRS), Campus de Luminy, Case 932, 13288 Marseille Cedex 09, France*

*3 - **Architecture et Fonction des Macromolécules Biologiques (AFMB,** UMR 6098), Aix-Marseille Univ., Campus de Luminy, Case 932, 13288 Marseille Cedex 09, France*

***Correspondence to Eric Cascales:** cascales@imm.cnrs.fr*
http://dx.doi.org/10.1016/j.jmb.2016.08.030
Edited by Bert Poolman

Abstract

The type VI secretion system (T6SS) is a multiprotein complex that delivers toxin effectors in both prokaryotic and eukaryotic cells. It is constituted of a long cytoplasmic structure—the tail—made of stacked Hcp hexamers and wrapped by a contractile sheath. Contraction of the sheath propels the inner tube capped by the VgrG spike protein toward the target cell. This tubular structure is built onto an assembly platform—the baseplate—that is composed of the TssEFGK-VgrG subunits. During the assembly process, the baseplate is recruited to a *trans*-envelope complex comprising the TssJ outer membrane lipoprotein and the TssL and TssM inner membrane proteins. This membrane complex serves as a docking station for the baseplate/tail and as a channel for the passage of the inner tube during sheath contraction. The baseplate is recruited to the membrane complex through multiple contacts including interactions of TssG and TssK with the cytoplasmic loop of TssM and of TssK with the cytoplasmic domain of TssL, $TssL_{Cyto}$. Here, we show that $TssL_{Cyto}$ interacts also with the TssE baseplate subunit. Based on the available $TssL_{Cyto}$ structures, we targeted conserved regions and specific features of $TssL_{Cyto}$ in enteroaggregative *Escherichia coli*. By using bacterial two-hybrid analysis and co-immunoprecipitation, we further show that the disordered L3–L4 loop is necessary to interact with TssK and that the L6–L7 loop mediates the interaction with TssE, whereas the TssM cytoplasmic loop binds the conserved groove of $TssL_{Cyto}$. Finally, competition assays demonstrated that these interactions are physiologically important for T6SS function.

Introduction

Bacteria have evolved strategies to survive within difficult environments or efficiently colonize a specific niche. When nutrients become limiting or when conditions are unfavorable, most Gram-negative Proteobacteria deliver antibacterial toxins into competitors. One of the main mechanisms for toxin delivery into prokaryotic cells is a multiprotein machinery called the type VI secretion system (T6SS) [1–6]. The T6SS resembles a ~600-nm long cytoplasmic tail-like tubular structure anchored to the cell envelope and works as a nano-crossbow [2,7,8]. The T6SS tail shares structural and functional homologies with contractile tail particles such as R-pyocins or bacteriophages [7–10]. The cytoplasmic tubular structure is constituted of an inner tube made of stacked Hcp hexamers organized head to tail and wrapped by a contractile sheath [7,9,11–17]. Contraction of the sheath propels the inner tube toward the target cell, allowing toxin delivery and target cell lysis [7,18–20]. This tubular structure is tipped by a spike composed of a trimer of the VgrG protein and of the PAAR protein, which serves as a puncturing device

Please cite this article as: A. Zoued, et al., Structure–Function Analysis of the TssL Cytoplasmic Domain Reveals a New Interaction between the Type VI Secretion Baseplate and Membrane ..., J. Mol. Biol. (2016), http://dx.doi.org/10.1016/j.jmb.2016.08.030

for penetration inside the target cell [9,21]. Toxin effectors are preloaded, and different mechanisms of transport have been proposed, including cargo models in which effectors directly or indirectly bind on VgrG or PAAR or within the lumen of Hcp hexamers [3,6,21–29].

The T6SS tail polymerizes on an assembly platform or baseplate complex (BC), which is also broadly conserved in contractile particles [30–34]. The composition of the T6SS baseplate has been recently revealed and is constituted the TssE, TssF, TssG, and TssK proteins that assemble a complex together with the VgrG spike [32,33,35]. Once assembled in the cytoplasm, the BC is recruited and stabilized by a *trans*-envelope complex,called the membrane complex (MC), constituted of TssJ, TssL, and TssM subunits [32,36,37]. The structure and assembly of the MC are well known. TssJ is an outer membrane lipoprotein with a transthyretin fold [38,39], whereas TssM and TssL are both anchored to the inner membrane. TssM is constituted of three transmembrane helices (TMH) that delimitate a cytoplasmic loop between TMH2 and TMH3 and a large periplasmic domain downstream of TMH3 [40,41]. This periplasmic domain could be segmented into four subdomains, with the C-terminal one mediating contacts with TssJ [37,39]. By contrast, TssL has a single TMH located at its extreme C terminus, and thus, the majority of the protein protrudes into the cytoplasm [42]. The structures of the TssL cytoplasmic domains of enteroaggregative *Escherichia coli* (EAEC), *Francisella tularensis*, and *Vibrio cholerae* have been reported: they are composed of seven helices grouped in two bundles, with an overall shape resembling a hook [43–45]. The biogenesis of the MC starts with TssJ at the outer membrane and progresses with the sequential addition of TssM and TssL [37]. Then, 10 copies of this heterotrimeric complex combine to assemble a 1.7-MDa *trans*-envelope complex that serves both as a docking station for the BC/tail structure and as a channel for the passage of the inner tube during sheath contraction [32,37,46]. Recruitment of the BC to the MC is mediated by multiple interactions including interactions of TssG and TssK with the cytoplasmic domain of TssM and of TssK with the cytoplasmic domain of TssL ($TssL_{Cyto}$) [32,41,47].

Here, we conducted a structure–function analysis of $TssL_{Cyto}$. We first demonstrate that in addition to making contacts with the cytoplasmic domain of TssM and TssK, $TssL_{Cyto}$ interacts with the TssE baseplate component. Comparison of the EAEC, *F. tularensis*, and *V. cholerae* $TssL_{Cyto}$ structures highlighted the presence of a cleft at the interface of the two-helix bundles with conserved negative charges. In addition, the two loops connecting helices 3–4 and 6–7 display significantly different shapes and/or flexibility. Site-directed mutagenesis coupled to protein–protein interaction studies demonstrated that the L3–4 and L6–7 loops mediate contact with the baseplate components TssK and TssE, respectively, whereas the central cleft accommodates the TssM cytoplasmic domain. Finally, antibacterial assays showed that all these contacts are necessary for proper function of the Type VI secretion apparatus.

Results

$TssL_{Cyto}$ interacts with itself, the cytoplasmic loop of TssM, and the TssE and TssK baseplate components

Previous studies have demonstrated that the cytoplasmic domain of the EAEC TssL protein [EC042_4527; Genbank accession (GI): 284924248] forms dimers and interacts with the TssM and TssK proteins [40,43,47]. To gain further insights onto the interaction network of $TssL_{Cyto}$, we performed a systematic bacterial two-hybrid (BACTH) analysis (Fig. 1a). As previously shown, we detected $TssL_{Cyto}$ interaction with itself, with TssK, and with the cytoplasmic domain of TssM ($TssM_{Cyto}$). In addition, this analysis revealed the interaction between $TssL_{Cyto}$ and the baseplate component TssE (Fig. 1a). The $TssL_{Cyto}$–TssE interaction was further validated *in vitro* by surface plasmon resonance (SPR) using purified proteins. TssE was covalently bound to the sensor chip, and recordings were monitored after injection of increasing concentrations of $TssL_{Cyto}$ (Fig. 1b and c). The sensorgrams confirmed the BACTH results and demonstrated that the two proteins interact with an affinity estimated to 55 ± 1.3 μM (Fig. 1b and c).

Structure analyses of TssL cytoplasmic domains

The crystal structures of the EAEC, *F. tularensis*, and *V. cholerae* TssL cytoplasmic domains are available (PDB IDs: 3U66 [43], 4ACL [44], and 4V3I [45]). All structures share common features (Fig. 2a and Supplementary Fig. S1): $TssL_{Cyto}$ is composed of seven α-helices organized in two bundles constituted of helices α1–4 and α5–7. The α5–7 bundle is made of shorter helices in average, making an overall hook-like structure delimiting a cleft comprising conserved charged residues including aspartate 74 and glutamate 75 (Supplementary Fig. S1A). However, the three structures also highlighted significant differences, notably in loops L3–L4 and L6–L7. The $TssL_{Cyto}$ loop L3–L4 is disordered in *F. tularensis* but comprises a small additional α-helix, αA, in EAEC and *V. cholerae*. In addition, part of the L3–L4 loop structure could not be solved in EAEC $TssL_{Cyto}$, suggesting that this loop exhibits structural flexibility. $TssL_{Cyto}$ loop L6–L7 comprises

Please cite this article as: A. Zoued, et al., Structure–Function Analysis of the TssL Cytoplasmic Domain Reveals a New Interaction between the Type VI Secretion Baseplate and Membrane ..., J. Mol. Biol. (2016), http://dx.doi.org/10.1016/j.jmb.2016.08.030

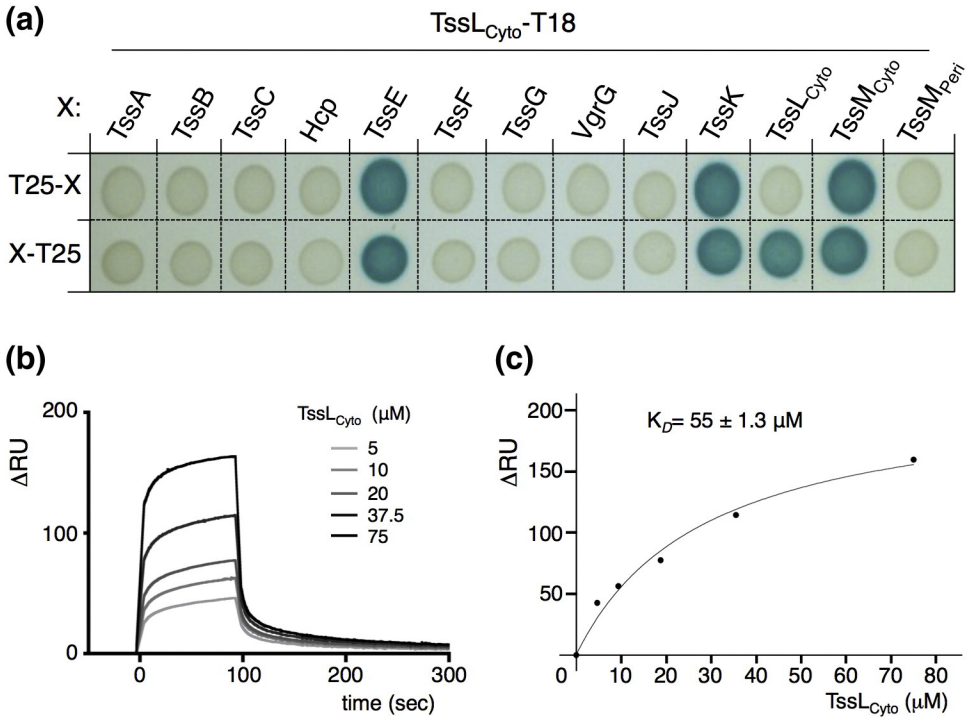

Fig. 1. TssL$_{Cyto}$ oligomerizes and interacts with TssE, TssK, and TssM$_{Cyto}$. (a) BACTH assay. BTH101 reporter cells producing the TssL$_{Cyto}$-T18 fusion protein and the indicated T6SS proteins fused to the T25 domain of the *Bordetella* adenylate cyclase were spotted on X-Gal-IPTG reporter LB agar plates. Only the cytoplasmic (Cyto) or periplasmic (Peri) domains were used for membrane-anchored proteins. (b and c) SPR analysis. (b) SPR sensorgrams (expressed as variation of resonance units, ΔRU) were recorded after injection of the increasing concentrations of purified TssL$_{Cyto}$ (from light gray to black: 5, 10, 20, 37.5, and 75 μM) on TssE-coated HC200m chips. (c) The graphs reporting ΔRU as a function of TssL$_{Cyto}$ concentration were used to estimate the dissociation constants of the TssL$_{Cyto}$–TssE complex.

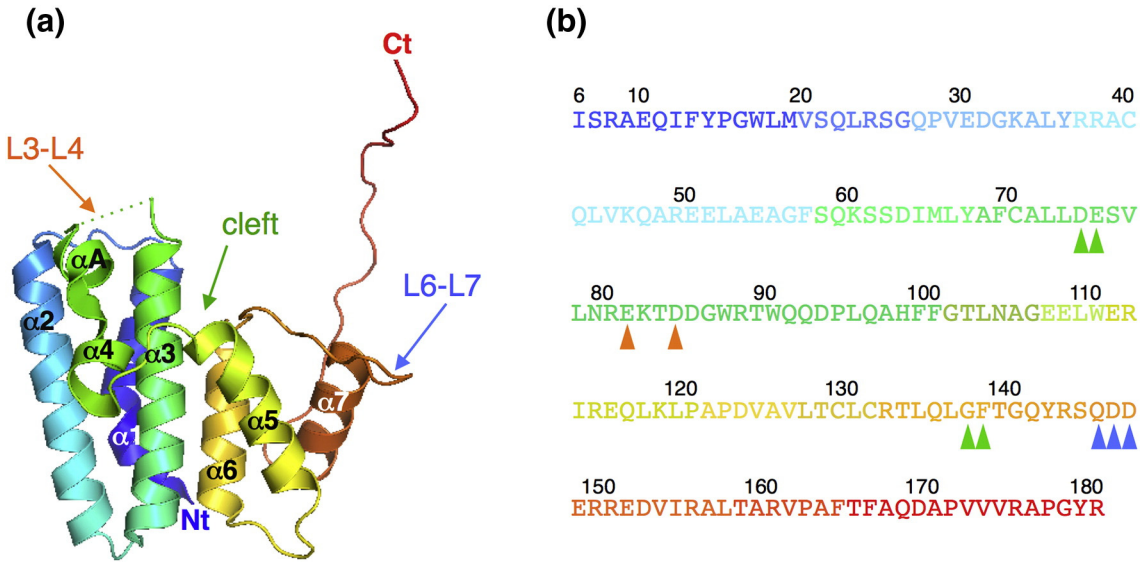

Fig. 2. Structure of the EAEC TssL$_{Cyto}$ domain. (a) Crystal structure of the EAEC TssL$_{Cyto}$ domain. The protein is shown as a ribbon, and α-helices (α1–α7) are indicated. The unstructured L3–L4 loop (orange arrow) is shown in dotted line, whereas the L6–L7 loop and the cleft are indicated by blue and green arrows, respectively. The figure was made with Chimera [56]. (b) Sequence of the crystallized TssL$_{Cyto}$ domain, with the same color code as in panel (a). The residues substituted in this study are indicated by arrowheads (green, cleft; orange, L3–L4 loop; blue, L6–L7 loop).

Please cite this article as: A. Zoued, et al., Structure–Function Analysis of the TssL Cytoplasmic Domain Reveals a New Interaction between the Type VI Secretion Baseplate and Membrane ..., J. Mol. Biol. (2016), http://dx.doi.org/10.1016/j.jmb.2016.08.030

an additional α-helix, αB, in *V. cholerae* but adopts different conformations in EAEC and *F. tularensis* (Supplementary Fig. S1). These two loops having distinct structures, conformations, or flexibility could be considered as interesting binding sites to confer specificity.

Mutagenesis of the charged cleft and the L3–L4 and L6–L7 loops unveils contact zones with $TssM_{Cyto}$, TssK, and TssE

To gain information on the role of the conserved cleft and the L3–L4 and L6–L7 loops, we engineered amino acid substitutions in these different regions (Fig. 2b and Table 1): (i) two charged residues (Glu-81 and Asp-84) within the loop L3–L4 were converted to opposed charges (GluAsp-to-LysLys mutant, called hereafter EKDK; orange arrows in Fig. 2); (ii) small (Gly-137), aromatic (Phe-138), and charged (Asp-74 and Glu-75) chains within the cleft were substituted to yield Gly-to-Glu (GE), Phe-to-Glu (FE), GlyPhe-to-GluGlu (GEFE), Asp-to-Arg (DR), Glu-to-Arg (ER), and AspGlu-to-ArgArg (DRER) mutants (green arrows in Fig. 2); and (iii) three hydrophilic/charged residues within the loop L6–L7 (Gln-145, Asp-146, and Asp-147) were substituted with lysine residues (GlnAspAsp-to-LysLysLys, QKDKDK; blue arrows in Fig. 2).

These substitutions were first introduced into the $TssL_{Cyto}$-T18 and pIBA-$TssL_{Cyto}$ vectors to test their impact on the interaction with TssE, TssK, and $TssM_{Cyto}$ using BACTH and co-immunoprecipitation (Fig. 3). Two-hybrid analyses showed that none of these substitutions break the oligomerization of $TssL_{Cyto}$ (Fig. 3a), in agreement with a previous study showing that $TssL_{Cyto}$ oligomerization is mediated by contacts between helices α1 [43]. These results also suggest that each mutant variant is properly produced and does not present large structural changes compared to the wild-type $TssL_{Cyto}$ domain. The assay also revealed that most mutations within the $TssL_{Cyto}$ central cleft prevent the formation of the $TssL_{Cyto}$–$TssM_{Cyto}$ complex, whereas substitutions within loops L3–L4 and L6–L7 abolish the interaction with TssK and TssE, respectively (Fig. 3a).

These two-hybrid results were validated by co-immunoprecipitation analyses. Soluble lysates of cells producing the C-terminally FLAG-tagged wild-type TssL cytoplasmic domain and its substitution variants were combined with lysates containing VSV-G-tagged TssE, TssK, and $TssM_{Cyto}$. $TssL_{Cyto}$-containing complexes were immobilized on agarose beads coupled to the monoclonal anti-FLAG antibody. Fig. 3b shows that the wild-type $TssL_{Cyto}$ domain co-precipitates TssE, TssK, and $TssM_{Cyto}$. Each $TssL_{Cyto}$ variant is produced and immunoprecipitated at levels comparable to the wild-type $TssL_{Cyto}$ domain. Mutation of the Glu-Asp (EKDK mutant) and Gln-Asp-Asp (QKDKDK mutant) motifs within the L3–L4 and L6–L7 loops prevented the interactions with TssK and TssE, respectively, whereas most substitutions within the conserved groove abolished the interaction with the TssM cytoplasmic domain (Fig. 3b).

$TssL_{Cyto}$ interactions with TssE, TssK, and $TssM_{Cyto}$ are critical for proper function of the type VI secretion apparatus

The EAEC Sci-1 T6SS is involved in interbacterial competition by delivering Tle1, a toxin with phospholipase activity, into competitor cells [27]. We therefore tested whether substitutions that abolish $TssL_{Cyto}$ complex formation impacted the function of the T6SS. The substitutions were introduced into the pOK-TssL vector that encodes the full-length TssL protein and was previously shown to fully complement the Δ*tssL* phenotypes [42]. The antibacterial activity was tested against a competitor strain engineered to constitutively produce the green fluorescent protein (GFP) and to resist kanamycin. The fluorescence levels of the mixture containing the EAEC and competitor strains, which is proportional to the number of competitor cells, were measured after 4 h of contact. In addition, the survival of the competitor strain was measured by counting the fluorescent colony-forming units after plating serial dilutions of the mixture on plates supplemented with kanamycin. The results represented in Fig. 4 show that the growth of the competitor strain was inhibited by the Δ*tssL* strain producing the wild-type TssL protein,

Table 1. Location of $TssL_{Cyto}$ substitutions

Mutant name	Amino–acid substitutions	Location	Interaction with:
EKDK	Glu–81–Lys, Asp84–Lys	L3–L4 loop	TssK
DR	Asp74–Arg	Cleft	TssMCyto
ER	Glu75–Arg	Cleft	TssMCyto
DRER	Asp74–Arg, Glu75–Arg	Cleft	TssMCyto
GE	Gly137–Glu	Cleft	TssMCyto
FE	Phe138–Glu	Cleft	None
GEFE	Gly137–Glu, Phe138–Glu	Cleft	TssMCyto
QKDKDK	Gln145–Lys, Asp146–Lys, Asp147–Lys	L6–L7 loop	TssE

Please cite this article as: A. Zoued, et al., Structure–Function Analysis of the TssL Cytoplasmic Domain Reveals a New Interaction between the Type VI Secretion Baseplate and Membrane ..., J. Mol. Biol. (2016), http://dx.doi.org/10.1016/j.jmb.2016.08.030

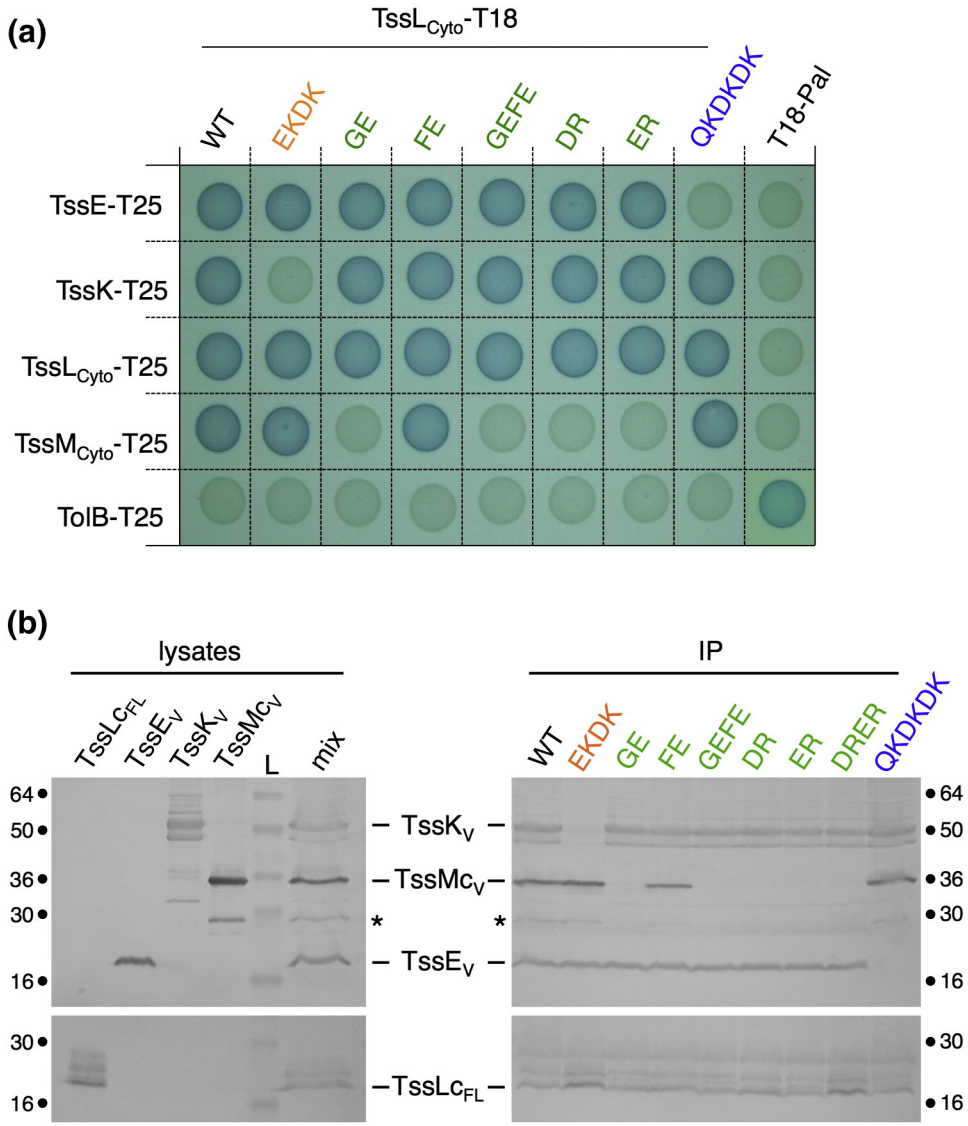

Fig. 3. Distinct motifs on TssL$_{Cyto}$ mediate interactions with TssE, TssK, and TssM$_{Cyto}$ (a) BACTH assay. BTH101 reporter cells producing the TssL$_{Cyto}$-T18 fusion protein variants and the indicated T6SS proteins or domains fused to the T25 domain of the *Bordetella* adenylate cyclase were spotted on X-Gal-IPTG reporter LB agar plates. (b) Co-immunoprecipitation assay. Soluble lysates from 3×10^{10} *E. coli* K12 W3110 cells producing wild-type (WT) or mutant FLAG-tagged TssL$_{Cyto}$ (TssLc$_{FL}$) and VSV-G-tagged TssE (TssE$_V$), TssK (TssK$_V$), or TssM$_{Cyto}$ (TssMc$_V$) proteins were subjected to immunoprecipitation with anti-FLAG-coupled beads. The lysates and immunoprecipitated (IP) material were separated by 12.5% acrylamide SDS-PAGE and immunodetected with anti-FLAG (lower panels) and anti-VSV-G (upper panels) monoclonal antibodies. Molecular weight markers (in kDa) are indicated.

at a level comparable to that of the wild-type strain. By contrast, the Δ*tssL* strain did not cause growth inhibition of competitor cells. With the exception of the FE mutant strain, all the TssL variants were unable to complement the antibacterial defects of the Δ*tssL* strain, demonstrating that formation of TssL$_{Cyto}$–TssE, TssL$_{Cyto}$–TssK, and TssL$_{Cyto}$–TssM$_{Cyto}$ complexes is necessary for proper assembly and function of the EAEC Sci-1 T6SS.

Discussion

In this study, we have used a systematic BACTH approach to define the partners of the T6SS TssL cytoplasmic domain. In addition to the known interacting subunits, TssM [40] and TssK [47], we have found an additional contact with the TssE protein, a component of the baseplate. This interaction was confirmed *in vitro* using SPR. With the

Please cite this article as: A. Zoued, et al., Structure–Function Analysis of the TssL Cytoplasmic Domain Reveals a New Interaction between the Type VI Secretion Baseplate and Membrane ..., J. Mol. Biol. (2016), http://dx.doi.org/10.1016/j.jmb.2016.08.030

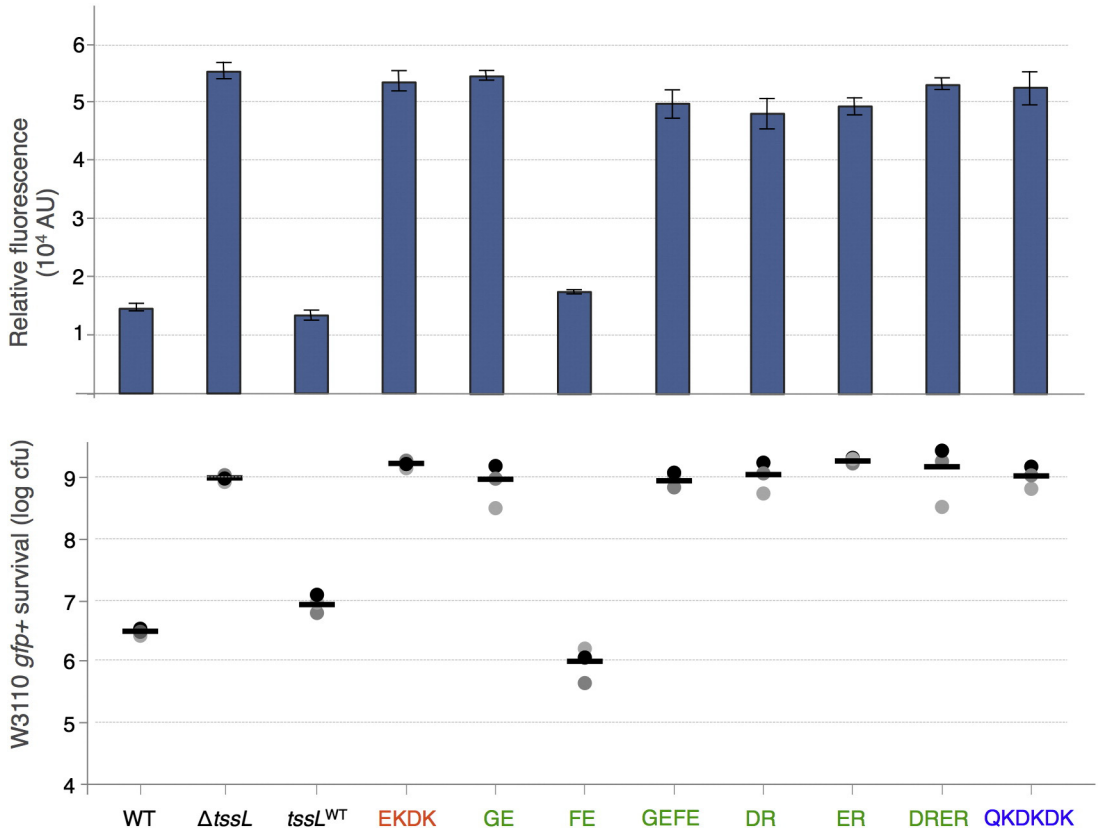

Fig. 4. $TssL_{Cyto}$ interactions with TssE, TssK, and $TssM_{Cyto}$ are required for T6SS antibacterial activity. *E. coli* K-12 prey cells (W3110 *gfp*$^+$, kan^R) were mixed with the indicated attacker cells, spotted onto Sci-1-inducing medium agar plates, and incubated for 4 h at 37 °C. The relative fluorescence of the bacterial mixture (in arbitrary unit or AU) is indicated in the upper graph, and the number of recovered *E. coli* prey cells (counted on selective kanamycin medium) is indicated in the graph (in log10 of colony-forming unit). The circles indicate the values from three independent assays, and the average is indicated by the bar.

identification of $TssM_{Cyto}$–TssG, $TssM_{Cyto}$–TssK, and $TssL_{Cyto}$–TssK contacts [32,41,47], the interaction of $TssL_{Cyto}$ with TssE corresponds to the fourth interaction described between the T6SS MC and BC complexes. The cytoplasmic domain of TssL is located at the base of the TssJLM complex [37], a location compatible with the position of the baseplate *in vivo* [7,32,48]. Although these interactions are of low affinity between isolated molecules (the dissociation constant measured *in vitro* for the $TssL_{Cyto}$–TssE interaction is ~50 μM), the avidity should increase within the secretion apparatus by the number of interactions and the local concentration. Furthermore, the existence of four contacts likely stabilizes the recruitment of the baseplate to the MC. These multiple contacts are probably important to properly position the baseplate onto the MC and to maintain the baseplate stably anchored when the sheath contracts. Indeed, it has been shown that the bacteriophage T4 baseplate is subjected to large conformational changes during sheath contraction [33,49], and a similar situation is likely to occur in the case of the T6SS [30,32]. Therefore, it might be critical to have a multitude of contacts between the BC and MC, as several interactions might be broken during the conformational transition.

TssL dimerizes and interacts with three proteins of the secretion apparatus (Fig. 5). In EAEC, TssL dimerization occurs mainly by the transmembrane segment with a contribution of residues from helix α1. In this study, we provided further molecular details on TssL interactions by conducting a structure–function analysis. First, using sequence alignment, we defined that a number of residues share a high level of conservation. Interestingly, most of these residues locate at the interface between the two-helix bundles and delimitate a cleft. Second, by comparing the three available crystal structures of TssL cytoplasmic domains (from EAEC, *F. tularensis*, and *V. cholerae*), we targeted two loops, loops L3–L4 and L6–L7, which present different shapes and distinct secondary structures (addition of short helices) and are highly degenerated. Substitutions were introduced in the cleft and in loops L3–L4 and L6–L7 and

Please cite this article as: A. Zoued, et al., Structure–Function Analysis of the TssL Cytoplasmic Domain Reveals a New Interaction between the Type VI Secretion Baseplate and Membrane ..., J. Mol. Biol. (2016), http://dx.doi.org/10.1016/j.jmb.2016.08.030

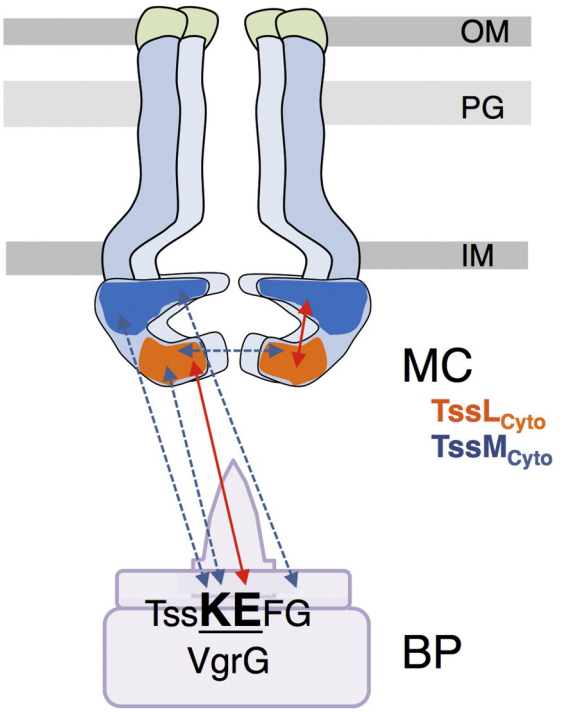

Fig. 5. Schematic representation of the TssL$_{Cyto}$ interaction network. Schematic representation of the TssJLM MC and its interactions with the TssKEFG–VgrG BC. The TssL (TssL$_{Cyto}$) and TssM (TssM$_{Cyto}$) cytoplasmic domains are shown in orange and blue, respectively. The interactions defined in this study are indicated by red arrows. Interactions determined previously [47] or in the accompanying article [41] are shown in blue dashed arrows.

were tested for their impact on the interactions. None of these mutations disrupted the oligomerization of TssL$_{Cyto}$, suggesting that their impact on TssL$_{Cyto}$ folding was null or moderated. Our data further show that the cleft is required for proper interaction with TssM$_{Cyto}$, whereas loops L3–L4 and L6–L7 are binding sites for TssK and TssE, respectively. The conservation of the charged crevice in TssL proteins suggests that the mode of binding of TssL/TssM proteins might be conserved. It is worthy to note that the T6SS-associated TssL and TssM proteins share homologies with IcmH/DotU and IcmF, two subunits of the *Legionella pneumophila* type IVb secretion system [8,43]. Interestingly, IcmH/DotU also possesses charged residues in the putative cleft position, suggesting that this cleft might also be important for binding to IcmF. By contrast, the variability of the L3–L4 and L6–L7 loops might confer specificity between the TssL proteins and the BC, notably when different T6SS are produced simultaneously in a bacterium. However, while our results demonstrate that these regions are necessary for these interactions, it remains to be defined whether these regions are sufficient. Swapping experiments between TssL proteins from different bacteria would be an interesting extension of this study. Finally, these data are interesting for the development of inhibitors that will target the assembly of the MC or the recruitment of the baseplate. Specifically, crevices, such as the cleft that accommodates the TssM cytoplasmic domain, are interesting targets for drugs, while mimetic peptides might be used to prevent the interaction of the baseplate components with the TssL loops.

Materials and Methods

Bacterial strains and media

The *E. coli* K-12 DH5α, BTH101, W3110, and BL21(DE3) pLysS strains were used for cloning procedures, BACTH analyses, co-immunoprecipitations, and protein production, respectively. Strain W3110 pUA66-*rrnB* (Kan^R, constitutively expressing the GFP) [50,51] was used as prey in antibacterial competition experiments. EAEC strain 17-2 has been used as source of DNA for PCR amplification and for phenotypic analyses. The Δ*tssL* 17-2 derivative mutant strain has been previously described [36]. Cells were grown in Lysogeny broth (LB), Terrific broth, or Sci-1-inducing medium [52] as specified. Plasmids were maintained by the addition of ampicillin (100 μg/mL), chloramphenicol (40 μg/mL), or kanamycin (50 μg/mL for *E. coli* K-12 and 100 μg/mL for EAEC). Expression of genes cloned into pOK12, pASK-IBA37+, pBAD33, and pETG20A vectors were induced by the addition of IPTG (50 μM in liquid, 10 μM on agar plates), anhydrotetracyclin (0.1 μg/mL), L-arabinose (0.2%), and IPTG (0.5 mM), respectively.

Plasmid construction

Plasmids used in this study are listed in Supplementary Table S1. PCRs were performed using a Biometra thermocycler using the Q5 high-fidelity DNA polymerase (New England BioLabs). Custom oligonucleotides, listed in Supplementary Table S1, were synthesized by Sigma Aldrich. EAEC 17–2 chromosomal DNA was used as a template for all PCRs. The amplified DNA fragments correspond to the full-length or the cytoplasmic domain (TssL$_{Cyto}$, residues 1–184) [42] of TssL (EC042_4527, GI: 284924248), the full-length TssK (EC042_4526, GI: 284924247) and TssE (EC042_4545, GI: 284924266) proteins, and the cytoplasmic domain (TssM$_{Cyto}$, residues 62–360) [41] of the TssM protein (EC042_4539, GI: 284924260). The pOK-TssL plasmid, producing the full-length TssL proteins fused to a C-terminal HA epitope, and plasmids pETG20A-TssL$_{Cyto}$ and pETG20A-TssE have been previously described [42,43,46]. The pASK-IBA37+ and pBAD33 plasmid derivatives, were engineered by restriction-free cloning [53] as previously described [36]. Briefly, genes of

interest were amplified with oligonucleotides introducing extensions annealing to the target vector. The double-stranded product of the first PCR was then used as oligonucleotides for a second PCR using the target vector as a template. Codon substitutions have been obtained by site-directed mutagenesis using complementary oligonucleotides bearing the nucleotide modifications. All constructs have been verified by restriction analysis and DNA sequencing (Eurofins, MWG).

BACTH assay

The adenylate cyclase-based BACTH technique [54] was used as previously published [55]. Briefly, compatible vectors producing proteins fused to the isolated T18 and T25 catalytic domains of the *Bordetella* adenylate cyclase were transformed into the reporter BTH101 strain, and the plates were incubated at 30 °C for 24 h. Three independent colonies for each transformation were inoculated into 600 μL of LB medium supplemented with ampicillin, kanamycin, and IPTG (0.5 mM). After overnight growth at 30 °C, 10 μL of each culture was spotted onto LB plates supplemented with ampicillin (100 μg/mL), kanamycin (50 μg/mL), IPTG (0.5 mM), and bromo-chloro-indolyl-β-D-galactopyranoside (40 μg/mL) and was incubated for 16 h at 30 °C. The experiments were done at least in triplicate from independent transformations, and a representative result is shown.

Co-immunoprecipitations

W3110 cells producing the protein of interest were grown to an A_{600} = ~0.4, and the expression of the cloned genes was induced with anhydrotetracyclin (0.1 μg/mL) or L-arabinose (0.2%) for 1 h. Then, 10^{10} cells were harvested, and the pellets were resuspended in 1 mL of LyticB buffer (Sigma-Aldrich) supplemented with 100 μg/mL lysozyme, 100 μg/mL DNase, and protease inhibitors (Complete, Roche) and were incubated for 20 min at 25 °C. Lysates were then clarified by centrifugation at 20,000*g* for 10 min. Then, 250 μL of each lysate were mixed and incubated for 30 min on a wheel, and the mixture was applied on anti-FLAG M2 affinity gel (Sigma-Aldrich). After 2 h of incubation, the beads were washed three times with 1 mL of 20 mM Tris–HCl (pH 7.5) and 100 mM NaCl, resuspended in 25 μL of Laemmli loading buffer, boiled for 10 min, and subjected to SDS-PAGE and immunodetection analyses.

Antibacterial competition assay

Antibacterial competition growth assays were performed as previously described in Sci-1-inducing conditions [27], except that the cultures were supplemented with 50 μM IPTG and that IPTG (10 μM) was added on the competition plates. The wild-type *E. coli* strain W3110 bearing the kanamycin-resistant GFP^+ pUA66-*rrnB* plasmid [51] was used as prey. After incubation on plates for 4 h, cells were scratched off, and the fluorescence levels were measured using a TECAN infinite M200 microplate reader. The number of surviving prey cells was measured by counting fluorescent colonies on kanamycin plates.

Protein purification

The TssE protein and TssL cytoplasmic domain produced from pETG20A derivatives are fused to an N-terminal 6× His-tagged thioredoxin (TRX), followed by a cleavage site for the tobacco etch virus protease. Purifications of TssE and $TssL_{Cyto}$ have been performed as previously described [43,46]. Briefly, *E. coli* BL21(DE3) pLysS cells carrying the pETG20A plasmid derivatives were grown at 37 °C in Terrific broth medium (1.2% peptone, 2.4% yeast extract, 72 mM K_2HPO_4, 17 mM KH_2PO_4, and 0.4% glycerol), and expression of the cloned genes was induced at A_{600} = 0.6 with 0.5 mM IPTG for 18 h at 16 °C. Cells were then resuspended in lysis buffer [50 mM Tris–HCl (pH 8.0), 300 mM NaCl, 1 mM EDTA, 0.5 mg/mL lysozyme, and 1 mM phenylmethylsulfonyl fluoride], submitted to four freeze-thawing cycles, and sonicated after the addition of 20 μg/mL DNase and 20 mM $MgCl_2$. The soluble fraction obtained after centrifugation for 30 min at 16,000*g* was loaded onto a 5-mL Nickel column (HisTrap™ FF) using an ÄKTA Explorer apparatus (GE healthcare), and the immobilized proteins were eluted in 50 mM Tris–HCl (pH 8.0) and 300 mM NaCl supplemented with 250 mM imidazole. The protein solution was desalted on a HiPrep 26/10 column (Sephadex™ G-25, Amersham Biosciences), and untagged proteins were obtained by cleavage using 2 mg of tobacco etch virus protease for 18 h at 4 °C and collected in the flow-through of a 5-mL Nickel column. The proteins were concentrated using the centricon technology (Millipore, 10-kDa cutoff). After concentration, the soluble proteins were passed through a Sephadex 200 26/60 column pre-equilibrated with 25 mM Tris–HCl (pH 7.5) and 100 mM NaCl, 5% Glycerol.

SPR

Steady-state interactions were monitored by SPR using a BIAcore T200 at 25 °C, as previously described [39]. Briefly, the HC200m sensor chip (Xantech) was coated with purified TRX-TssE fusion protein immobilized by amine coupling (ΔRU = 4000–4300). A control flow cell was coated with TRX immobilized by amine coupling at the same concentration (ΔRU = 4100). Purified $TssL_{Cyto}$ (five concentrations ranging from 5 to 75 μM) were injected, and binding traces were recorded in duplicate. The signal from the control flow cell and the buffer response were subtracted from

Please cite this article as: A. Zoued, et al., Structure–Function Analysis of the TssL Cytoplasmic Domain Reveals a New Interaction between the Type VI Secretion Baseplate and Membrane ..., J. Mol. Biol. (2016), http://dx.doi.org/10.1016/j.jmb.2016.08.030

all measurements. The dissociation constants, K_D, were estimated using the GraphPad Prism 5.0 software on the basis of the steady-state levels of ΔRU, which are directly related to the concentration of the analytes. The K_D were estimated by plotting the different ΔRU at a fixed time (5 s before the end of the injection step) against the different concentrations of $TssL_{Cyto}$. For K_D calculation, the nonlinear regression fit for XY analysis, and one site (specific binding) as a model, which corresponds to the equation $Y = Bmax^*X/(K_d + X)$, were used.

The supplementary information contains one Supplementary Table (Strains, plasmids, and oligonucleotides used in this study) and two Supplementary Figures (S1, Comparison of the EAEC, *F. tularensis*, and *V. cholerae* $TssL_{Cyto}$ structures; and S2, Sequence alignment of TssL proteins). Supplementary data associated with this article can be found in the online version at http://dx.doi.org/10.1016/j.jmb.2016.08.030.

Acknowledgments

We thank Laetitia Houot and Bérengère Ize and the members of the Cascales, Cambillau, Lloubès, Bouveret, and Sturgis research groups for insightful discussions; Annick Brun, Isabelle Bringer, and Olivier Uderso for technical assistance; and Marc Assin for encouragements. This work was supported by the Centre Nationale de la Recherche Scientifique (CNRS), the Aix-Marseille Université (AMU), and Agence Nationale de la Recherche (ANR) and Fondation pour la Recherche Médicale (FRM) research grants (ANR-10-JCJC-1303-03 and ANR-14-CE14-0006-02, DEQ2011-0421282). A.Z. was a recipient of a Ministère de la Recherche doctoral and FRM end-of-thesis (FDT20140931060) fellowships.

The authors declare no competing financial interests.

Authors contributions: A.Z., A.P.E., and L.J. constructed the vectors for the *in vivo* studies and performed the BACTH experiments, C.J.C. performed the co-immunoprecipitations and antibacterial assays; A.Z., E.D., and E.C. analyzed the TssL structure and identified the regions for mutagenesis. B.D. purified TssE and performed SPR experiments. C.C. and E.C. supervised the experiments. E.C. wrote the manuscript. Each author reviewed the manuscript prior to submission.

Received 1 August 2016;
Received in revised form 29 August 2016;
Accepted 30 August 2016
Available online xxxx

Keywords:
type VI secretion;
protein–protein interaction;
membrane complex;
baseplate complex;

Present address: Howard Hughes Medical Institute, Brigham and Women's Hospital, Division of Infectious Diseases and Harvard Medical School, Department of Microbiology and Immunobiology, Boston, MA 02115, USA.

Present address: Laboratoire d'Ingénierie des Systèmes Macromoléculaires (LISM, UMR 7255), Institut de Microbiologie de la Méditerranée (IMM), Aix-Marseille Univ. - Centre National de la Recherche Scientifique (CNRS), 31 Chemin Joseph Aiguier, 13402 Marseille Cedex 20, France.

Present address: Technological Advances for Genomics and Clinics laboratory (TAGC, U1090), Aix-Marseille Univ. - Institut National de la Santé et de la Recherche Médicale (INSERM), 163 Avenue de Luminy, 13288 Marseille Cedex 09, France.

Abbreviations used:
T6SS, type VI secretion system; BC, baseplate complex; MC, membrane complex; TMH, transmembrane helices; EAEC, enteroaggregative *Escherichia coli*; $TssL_{Cyto}$, cytoplasmic domain of TssL; GI, Genbank accession; BACTH, bacterial two-hybrid; $TssM_{Cyto}$, cytoplasmic domain of TssM; SPR, surface plasmon resonance; GFP, green fluorescent protein; LB, Lysogeny broth; TRX, thioredoxin.

References

[1] S.J. Coulthurst, The type VI secretion system—a widespread and versatile cell targeting system, Res. Microbiol. 164 (2013) 640–654.
[2] A. Zoued, Y.R. Brunet, E. Durand, M.S. Aschtgen, L. Logger, B. Douzi, L. Journet, C. Cambillau, E. Cascales, Architecture and assembly of the type VI secretion system, Biochim. Biophys. Acta 1843 (2014) 1664–1673.
[3] E. Durand, C. Cambillau, E. Cascales, L. Journet, VgrG, Tae, Tle, and beyond: the versatile arsenal of type VI secretion effectors, Trends Microbiol. 22 (2014) 498–507.
[4] B.T. Ho, T.G. Dong, J.J. Mekalanos, A view to a kill: the bacterial type VI secretion system, Cell Host Microbe 15 (2014) 9–21.
[5] M. Basler, Type VI secretion system: secretion by a contractile nanomachine, Philos. Trans. R. Soc. Lond. Ser. B Biol. Sci. 370 (2015) 1679.
[6] J. Alcoforado Diniz, Y.C. Liu, S.J. Coulthurst, Molecular weaponry: diverse effectors delivered by the type VI secretion system, Cell. Microbiol. 17 (2015) 1742–1751.
[7] M. Basler, M. Pilhofer, G.P. Henderson, G.J. Jensen, J.J. Mekalanos, Type VI secretion requires a dynamic contractile phage tail-like structure, Nature 483 (2012) 182–186.
[8] E. Cascales, C. Cambillau, Structural biology of type VI secretion systems, Philos. Trans. R. Soc. Lond. Ser. B Biol. Sci. 367 (2012) 1102–1111.
[9] P.G. Leiman, M. Basler, U.A. Ramagopal, J.B. Bonanno, J.M. Sauder, S. Pukatzki, S.K. Burley, S.C. Almo, J.J. Mekalanos, Type VI secretion apparatus and phage tail-associated protein complexes share a common evolutionary origin, Proc. Natl. Acad. Sci. U. S. A. 106 (2009) 4154–4159.

Please cite this article as: A. Zoued, et al., Structure–Function Analysis of the TssL Cytoplasmic Domain Reveals a New Interaction between the Type VI Secretion Baseplate and Membrane ..., J. Mol. Biol. (2016), http://dx.doi.org/10.1016/j.jmb.2016.08.030

[10] G. Bönemann, A. Pietrosiuk, A. Mogk, Tubules and donuts: a type VI secretion story, Mol. Microbiol. 76 (2010) 815–821.
[11] J.D. Mougous, M.E. Cuff, S. Raunser, A. Shen, M. Zhou, C.A. Gifford, A.L. Goodman, G. Joachimiak, C.L. Ordoñez, S. Lory, T. Walz, A. Joachimiak, J.J. Mekalanos, A virulence locus of *Pseudomonas aeruginosa* encodes a protein secretion apparatus, Science 312 (2006) 1526–1530.
[12] E.R. Ballister, A.H. Lai, R.N. Zuckermann, Y. Cheng, J.D. Mougous, *In vitro* self-assembly of tailorable nanotubes from a simple protein building block, Proc. Natl. Acad. Sci. U. S. A. 105 (2008) 3733–3738.
[13] N.S. Lossi, E. Manoli, A. Förster, R. Dajani, T. Pape, P. Freemont, A. Filloux, The HsiB1C1 (TssB–TssC) complex of the *Pseudomonas aeruginosa* type VI secretion system forms a bacteriophage tail sheathlike structure, J. Biol. Chem. 288 (2013) 7536–7548.
[14] Y.R. Brunet, J. Hénin, H. Celia, E. Cascales, Type VI secretion and bacteriophage tail tubes share a common assembly pathway, EMBO Rep. 15 (2014) 315–321.
[15] B. Douzi, S. Spinelli, S. Blangy, A. Roussel, E. Durand, Y.R. Brunet, E. Cascales, C. Cambillau, Crystal structure and self-interaction of the type VI secretion tail-tube protein from enteroaggregative *Escherichia coli*, PLoS One 9 (2014), e86918.
[16] X.Y. Zhang, Y.R. Brunet, L. Logger, B. Douzi, C. Cambillau, L. Journet, E. Cascales, Dissection of the TssB–TssC interface during type VI secretion sheath complex formation, PLoS One 8 (2013), e81074.
[17] M. Kudryashev, R.Y. Wang, M. Brackmann, S. Scherer, T. Maier, D. Baker, F. DiMaio, H. Stahlberg, E.H. Egelman, M. Basler, Structure of the type VI secretion system contractile sheath, Cell 160 (2015) 952–962.
[18] M. LeRoux, J.A. De Leon, N.J. Kuwada, A.B. Russell, D. Pinto-Santini, R.D. Hood, D.M. Agnello, S.M. Robertson, P.A. Wiggins, J.D. Mougous, Quantitative single-cell characterization of bacterial interactions reveals type VI secretion is a double-edged sword, Proc. Natl. Acad. Sci. U. S. A. 109 (2012) 19,804–19,809.
[19] M. Basler, B.T. Ho, J.J. Mekalanos, Tit-for-tat: type VI secretion system counterattack during bacterial cell–cell interactions, Cell 152 (2013) 884–894.
[20] Y.R. Brunet, L. Espinosa, S. Harchouni, T. Mignot, E. Cascales, Imaging type VI secretion-mediated bacterial killing, Cell Rep. 3 (2013) 36–41.
[21] M.M. Shneider, S.A. Buth, B.T. Ho, M. Basler, J.J. Mekalanos, P.G. Leiman, PAAR-repeat proteins sharpen and diversify the type VI secretion system spike, Nature 500 (2013) 350–353.
[22] S. Pukatzki, A.T. Ma, A.T. Revel, D. Sturtevant, J.J. Mekalanos, Type VI secretion system translocates a phage tail spike-like protein into target cells where it cross-links actin, Proc. Natl. Acad. Sci. U. S. A. 104 (2007) 15,508–15,513.
[23] J.M. Silverman, D.M. Agnello, H. Zheng, B.T. Andrews, M. Li, C.E. Catalano, T. Gonen, J.D. Mougous, Haemolysin coregulated protein is an exported receptor and chaperone of type VI secretion substrates, Mol. Cell 51 (2013) 584–593.
[24] T.G. Sana, N. Flaugnatti, K.A. Lugo, L.H. Lam, A. Jacobson, V. Baylot, E. Durand, L. Journet, E. Cascales, D.M. Monack, Salmonella Typhimurium utilizes a T6SS-mediated antibacterial weapon to establish in the host gut, Proc. Natl. Acad. Sci. U. S. A. 113 (2016) 5044–5051.
[25] D. Unterweger, B. Kostiuk, R. Ötjengerdes, A. Wilton, L. Diaz-Satizabal, S. Pukatzki, Chimeric adaptor proteins translocate diverse type VI secretion system effectors in *Vibrio cholerae*, EMBO J. 34 (2015) 2198–2210.
[26] X. Liang, R. Moore, M. Wilton, M.J. Wong, L. Lam, T.G. Dong, Identification of divergent type VI secretion effectors using a conserved chaperone domain, Proc. Natl. Acad. Sci. U. S. A. 112 (2016) 9106–9111.
[27] N. Flaugnatti, T.T. Le, S. Canaan, M.S. Aschtgen, V.S. Nguyen, S. Blangy, C. Kellenberger, A. Roussel, C. Cambillau, E. Cascales, L. Journet, A phospholipase A1 anti-bacterial T6SS effector interacts directly with the C-terminal domain of the VgrG spike protein for delivery, Mol. Microbiol. 99 (2016) 1099–1118.
[28] D.D. Bondage, J.S. Lin, L.S. Ma, C.H. Kuo, E.M. Lai, VgrG C terminus confers the type VI effector transport specificity and is required for binding with PAAR and adaptor-effector complex, Proc. Natl. Acad. Sci. U. S. A. 113 (2016) 3931–3940.
[29] F.R. Cianfanelli, J. Alcoforado Diniz, M. Guo, V. De Cesare, M. Trost, S.J. Coulthurst, VgrG and PAAR proteins define distinct versions of a functional type VI secretion system, PLoS Pathog. 12 (2016), e1005735.
[30] P.G. Leiman, M.M. Shneider, Contractile tail machines of bacteriophages, Adv. Exp. Med. Biol. 726 (2012) 93–114.
[31] P.F. Sarris, E.D. Ladoukakis, N.J. Panopoulos, E.V. Scoulica, A phage tail-derived element with wide distribution among both prokaryotic domains: a comparative genomic and phylogenetic study, Genome Biol. Evol. 6 (2014) 1739–1747.
[32] Y.R. Brunet, A. Zoued, F. Boyer, B. Douzi, E. Cascales, The type VI secretion TssEFGK-VgrG phage-like baseplate is recruited to the TssJLM membrane complex via multiple contacts and serves as assembly platform for tail tube/sheath polymerization, PLoS Genet. 11 (2015), e1005545.
[33] N.M. Taylor, N.S. Prokhorov, R.C. Guerrero-Ferreira, M.M. Shneider, C. Browning, K.N. Goldie, H. Stahlberg, P.G. Leiman, Structure of the T4 baseplate and its function in triggering sheath contraction, Nature 533 (2016) 346–352.
[34] A. Filloux, P. Freemont, Structural biology: baseplates in contractile machines, Nat. Microbiol. 1 (2016) 16104.
[35] G. English, O. Byron, F.R. Cianfanelli, A.R. Prescott, S.J. Coulthurst, Biochemical analysis of TssK, a core component of the bacterial type VI secretion system, reveals distinct oligomeric states of TssK and identifies a TssK–TssFG subcomplex, Biochem. J. 461 (2014) 291–304.
[36] M.S. Aschtgen, M. Gavioli, A. Dessen, R. Lloubès, E. Cascales, The SciZ protein anchors the enteroaggregative *Escherichia coli* type VI secretion system to the cell wall, Mol. Microbiol. 75 (2010) 886–899.
[37] E. Durand, V.S. Nguyen, A. Zoued, L. Logger, G. Péhau-Arnaudet, M.S. Aschtgen, S. Spinelli, A. Desmyter, B. Bardiaux, A. Dujeancourt, A. Roussel, C. Cambillau, E. Cascales, R. Fronzes, Biogenesis and structure of a type VI secretion membrane core complex, Nature 523 (2015) 555–560.
[38] M.S. Aschtgen, C.S. Bernard, S. De Bentzmann, R. Lloubès, E. Cascales, SciN is an outer membrane lipoprotein required for type VI secretion in enteroaggregative *Escherichia coli*, J. Bacteriol. 190 (2008) 7523–7531.
[39] C. Felisberto-Rodrigues, E. Durand, M.S. Aschtgen, S. Blangy, M. Ortiz-Lombardia, B. Douzi, C. Cambillau, E. Cascales, Towards a structural comprehension of bacterial type VI secretion systems: characterization of the TssJ–TssM complex of an *Escherichia coli* pathovar, PLoS Pathog. 7 (2011), e1002386.
[40] L.S. Ma, J.S. Lin, E.M. Lai, An IcmF family protein, ImpLM, is an integral inner membrane protein interacting with ImpKL,

Please cite this article as: A. Zoued, et al., Structure–Function Analysis of the TssL Cytoplasmic Domain Reveals a New Interaction between the Type VI Secretion Baseplate and Membrane ..., J. Mol. Biol. (2016), http://dx.doi.org/10.1016/j.jmb.2016.08.030

and its walker a motif is required for type VI secretion system-mediated Hcp secretion in *Agrobacterium tumefaciens*, J. Bacteriol. 191 (2009) 4316–4329.

[41] L. Logger, M.S. Aschtgen, M. Guérin, E. Cascales, E. Durand, Molecular dissection of the interface between the type VI secretion TssM cytoplasmic domain and the TssG baseplate component, J. Mol. Biol. (2016).

[42] M.S. Aschtgen, A. Zoued, R. Lloubès, L. Journet, E. Cascales, The C-tail anchored TssL subunit, an essential protein of the enteroaggregative *Escherichia coli* Sci-1 type VI secretion system, is inserted by YidC, Microbiologyopen 1 (2012) 71–82.

[43] E. Durand, A. Zoued, S. Spinelli, P.J. Watson, M.S. Aschtgen, L. Journet, C. Cambillau, E. Cascales, Structural characterization and oligomerization of the TssL protein, a component shared by bacterial type VI and type IVb secretion systems, J. Biol. Chem. 287 (2012) 14,157–14,168.

[44] C.S. Robb, F.E. Nano, A.B. Boraston, The structure of the conserved type six secretion protein TssL (DotU) from *Francisella novicida*, J. Mol. Biol. 419 (2012) 277–283.

[45] J.H. Chang, Y.G. Kim, Crystal structure of the bacterial type VI secretion system component TssL from *Vibrio cholerae*, J. Microbiol. 53 (2015) 32–37.

[46] A. Zoued, E. Durand, Y.R. Brunet, S. Spinelli, B. Douzi, M. Guzzo, N. Flaugnatti, P. Legrand, L. Journet, R. Fronzes, T. Mignot, C. Cambillau, E. Cascales, Priming and polymerization of a bacterial contractile tail structure, Nature 531 (2016) 59–63.

[47] A. Zoued, E. Durand, C. Bebeacua, Y.R. Brunet, B. Douzi, C. Cambillau, E. Cascales, L. Journet, TssK is a trimeric cytoplasmic protein interacting with components of both phage-like and membrane anchoring complexes of the type VI secretion system, J. Biol. Chem. 288 (2013) 27,031–27,041.

[48] A.J. Gerc, A. Diepold, K. Trunk, M. Porter, C. Rickman, J.P. Armitage, N.R. Stanley-Wall, S.J. Coulthurst, Visualization of the *serratia* type VI secretion system reveals unprovoked attacks and dynamic assembly, Cell Rep. 12 (2015) 2131–2142.

[49] V.A. Kostyuchenko, P.G. Leiman, P.R. Chipman, S. Kanamaru, M.J. van Raaij, F. Arisaka, V.V. Mesyanzhinov, M.G. Rossmann, Three-dimensional structure of bacteriophage T4 baseplate, Nat. Struct. Biol. 10 (2003) 688–693.

[50] E. Gueguen, E. Cascales, Promoter swapping unveils the role of the *Citrobacter rodentium* CTS1 type VI secretion system in interbacterial competition, Appl. Environ. Microbiol. 79 (2013) 32–38.

[51] A. Zaslaver, A. Bren, M. Ronen, S. Itzkovitz, I. Kikoin, S. Shavit, W. Liebermeister, M.G. Surette, U. Alon, A comprehensive library of fluorescent transcriptional reporters for *Escherichia coli*, Nat. Methods 3 (2006) 623–628.

[52] Y.R. Brunet, C.S. Bernard, M. Gavioli, R. Lloubès, E. Cascales, An epigenetic switch involving overlapping fur and DNA methylation optimizes expression of a type VI secretion gene cluster, PLoS Genet. 7 (2011), e1002205.

[53] F. van den Ent, J. Löwe, RF cloning: a restriction-free method for inserting target genes into plasmids, J. Biochem. Biophys. Methods 67 (2006) 67–74.

[54] G. Karimova, J. Pidoux, A. Ullmann, D. Ladant, A bacterial two-hybrid system based on a reconstituted signal transduction pathway, Proc. Natl. Acad. Sci. U. S. A. 95 (1998) 5752–5756.

[55] A. Battesti, E. Bouveret, The bacterial two-hybrid system based on adenylate cyclase reconstitution in *Escherichia coli*, Methods 58 (2012) 325–334.

[56] E.F. Pettersen, T.D. Goddard, C.C. Huang, G.S. Couch, D.M. Greenblatt, E.C. Meng, T.E. Ferrin, UCSF chimera—a visualization system for exploratory research and analysis, J. Comput. Chem. 25 (2004) 1605–1612.

Please cite this article as: A. Zoued, et al., Structure–Function Analysis of the TssL Cytoplasmic Domain Reveals a New Interaction between the Type VI Secretion Baseplate and Membrane ..., J. Mol. Biol. (2016), http://dx.doi.org/10.1016/j.jmb.2016.08.030